Overview of recent observations and simulations from the American WAKE experimeNt (AWAKEN) field campaign

Patrick Moriarty[1], Nicola Bodini[1], Lawrence Cheung,[2], Nicholas Hamilton[1], Thomas Herges[3], Colleen Kaul[4], Stefano Letizia[1], Mikhail Pekour[4], and Eric Simley[1]

[1]National Renewable Energy Laboratory, Golden, CO 80401, USA
[2]Sandia National Laboratories, Livermore, CA 94551, USA
[3]Sandia National Laboratories, Albuquerque, NM 87175, USA
[4]Pacific Northwest National Laboratory, Richland, WA 99354, USA

E-mail: patrick.moriarty@nrel.gov

Abstract. The American WAKE experimeNt (AWAKEN) is a large-scale field campaign focused on gathering new detailed observations of wind farm–atmosphere interactions for improved understanding of wind farm physics and overall performance. The field campaign, centered around five wind farms in northern Oklahoma, began in September 2022 and will run through at least October 2023. This paper summarizes some of the initial observations and simulations performed as part of the AWAKEN project.

1. Introduction

The focus of the American WAKE experimeNt (AWAKEN) project is centered around observations and companion simulations relevant for seven testable hypotheses [1] geared toward improved understanding of individual turbine wakes, turbulence within wind farms, larger-scale wind farm wakes, wind farm blockage and the impacts of dynamic atmospheric events and turbine operation on power production and turbine structural loads. The campaign includes a variety of instruments deployed at 13 unique field sites and on four wind turbines in northern Oklahoma. Most instruments are placed in and around a single wind farm (King Plains), but some field sites are located in other wind farms in the area to capture larger-scale phenomena such as wind farm wake interactions. In addition to observing the atmospheric flow fields, structural loading information is being gathered from a suite of sensors installed on three turbines in the King Plains wind farm. Researchers are also modifying the operational strategies of subsets of turbines within the King Plains wind farm to quantify the impact of two different types of wind farm control on wind farm performance and reliability.

In conjunction with the ongoing observations of the AWAKEN campaign, researchers are executing complementary simulations using multiple tools with varying levels of fidelity. The suite of simulations includes some of the highest fidelity wind farm models run to date using the ExaWind simulation environment [2] and also lower fidelity engineering models important for quick estimates of wind farm power production and control systems design, such as FLORIS

[3]. The goals of the simulations are to help design the wind farm controls aspects of the experiment and to perform validation studies to quantify the accuracy of models used to predict flow fields and energy production under a variety of atmospheric and wind farm operational conditions. Such simulations used in conjunction with observations will also provide improved understanding of wind farm flow physics that continue to be a significant source of uncertainty for wind farm energy prediction [4]. Researchers will use these simulations and observations to create a set of publicly available benchmarks that will be valuable for the international wind energy community.

In this paper, we provide a summary of the experimental setup in Section 2. We then summarize some preliminary results from observational analysis and simulations in Sections 3 and 4, respectively, and provide conclusions in Section 5.

2. Experimental setup

The field sites located around three of the wind farms in the AWAKEN project are shown in figure 1, with an enlarged view of the King Plains sites and instrumented turbines shown on the right. The dominant wind direction is southerly [5], which dictates the experimental layout of transects running north south through the King Plains wind farm to observe how different atmospheric quantities vary as the wind flows through and out of the wind farm. Details of the instrumentation deployed and the philosophy behind the field campaign design can be found in Moriarty et al. [6].

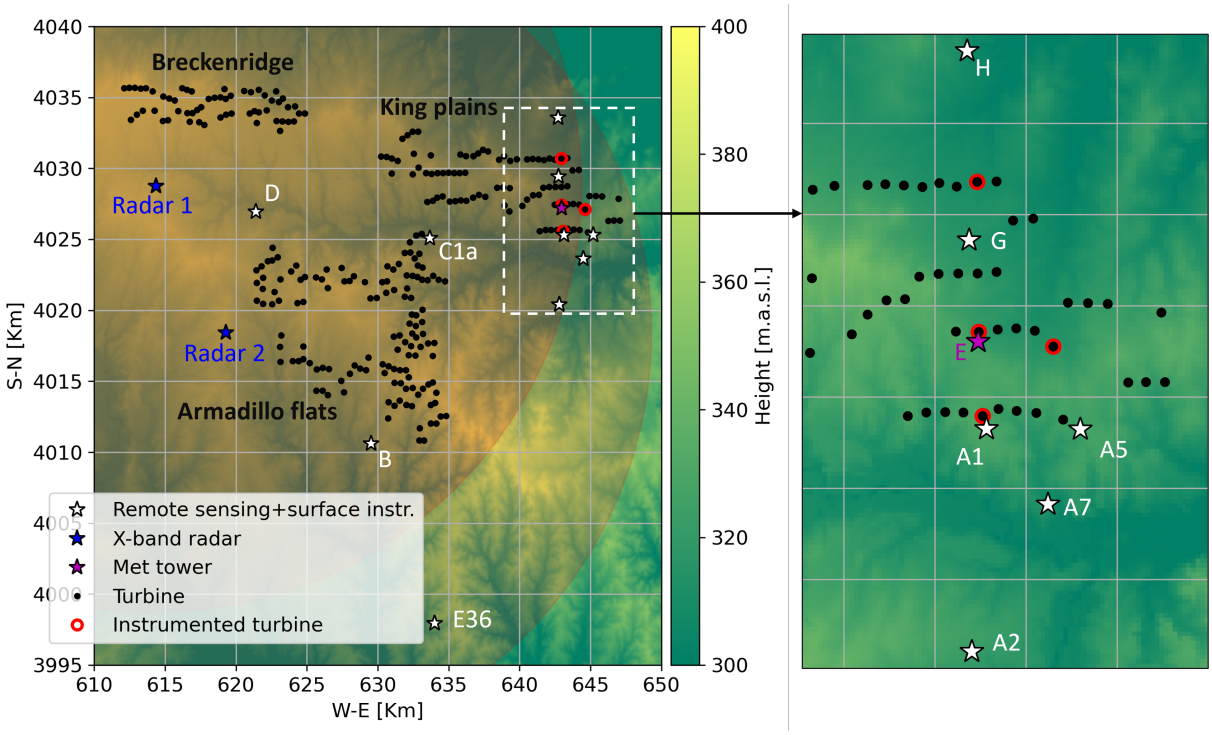

Figure 1. Layout of the AWAKEN instrumented sites. Black dots represent wind turbines and black dots with red circles represent the AWAKEN instrumented turbines. Orange partial circles on the left represent the range of the X-band radars.

3. Observations

Initial observations from the AWAKEN experiment presented in this paper are from ground-based profiling and scanning lidars and surface stations with sonic anemometers located either upwind, within, or downwind of the King Plains wind farm, depending on the observed wind direction.

The ground-based scanning lidars installed at sites A1 and H perform a six-beam vertical profiling scan sequence [7] for the characterization of the first- and second-order statistics of the wind velocity field as a function of height, z. Similar vertical profiles can be retrieved from the profiling lidar deployed at site B. Wind speed and direction from these three lidars during one selected day are reported in figure 2. All the instruments indicate the same mesoscale forcing, with highly sheared NNW winds between 0000 and 0300 UTC (6–9 p.m. local time), shifting to a westerly flow around 1200 UTC (6 a.m. local time). The nighttime wind speed at site A1 (0600–1200 UTC) exhibits lower values compared to the other two lidars below 200 m, which represent a clear signature of turbine wakes that are expected to impact site A1 for wind blowing from the north.

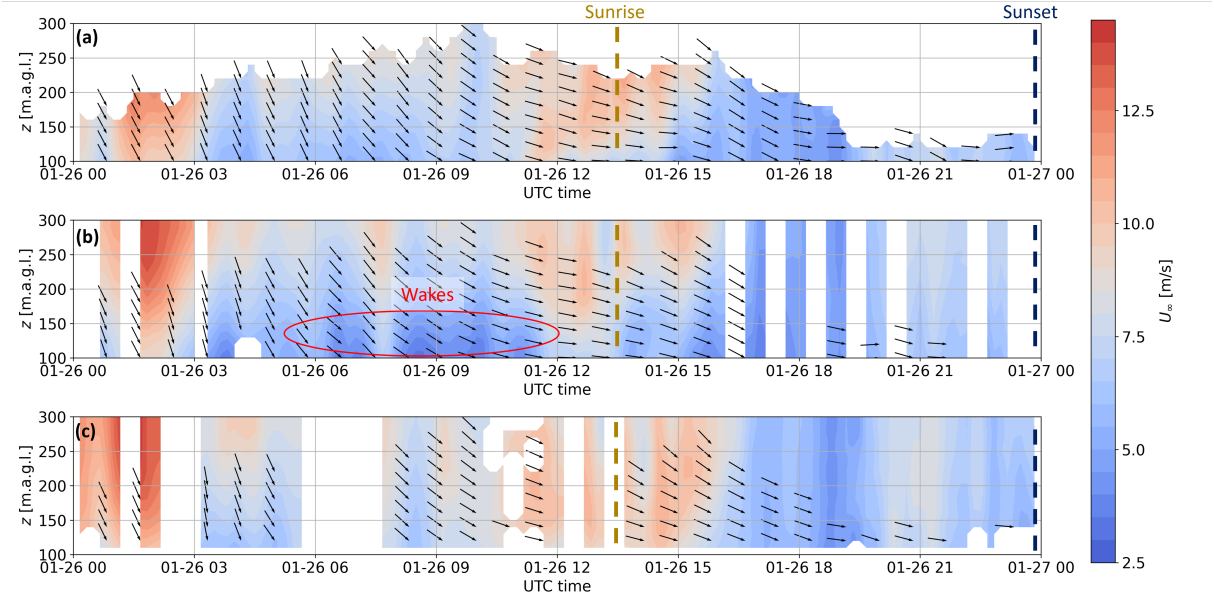

Figure 2. (a) 10-minute-averaged time-height cross sections of wind speed retrieved from the site B Windcube profiling lidar, (b) Halo XR+ scanning lidar at site A1, and (c) Halo XR+ scanning lidar at site H. The black arrows indicate the 10-minute-averaged wind direction. Blank areas correspond to data rejected after the quality check based on [8], with the inconsistent data availability being related to different lidar models and/or local aerosol conditions.

We also evaluate the lidar-derived turbulence kinetic energy (TKE) at a few selected heights and compare it to its equivalent calculated from the 4-m sonic anemometer at site A2 (figure 3). A clear diurnal cycle can be observed both near the ground and aloft, with lower values occurring in the first half of the day (nighttime, stable conditions) and higher turbulence level in the second half (daytime, unstable convective conditions). It is noteworthy that the lidar at site A1, i.e., the one more severely affected by wakes for the wind directions sampled here, senses a TKE as high as 2–3 times that of the lidar at site H, which is interpreted as an effect of wake-added turbulence.

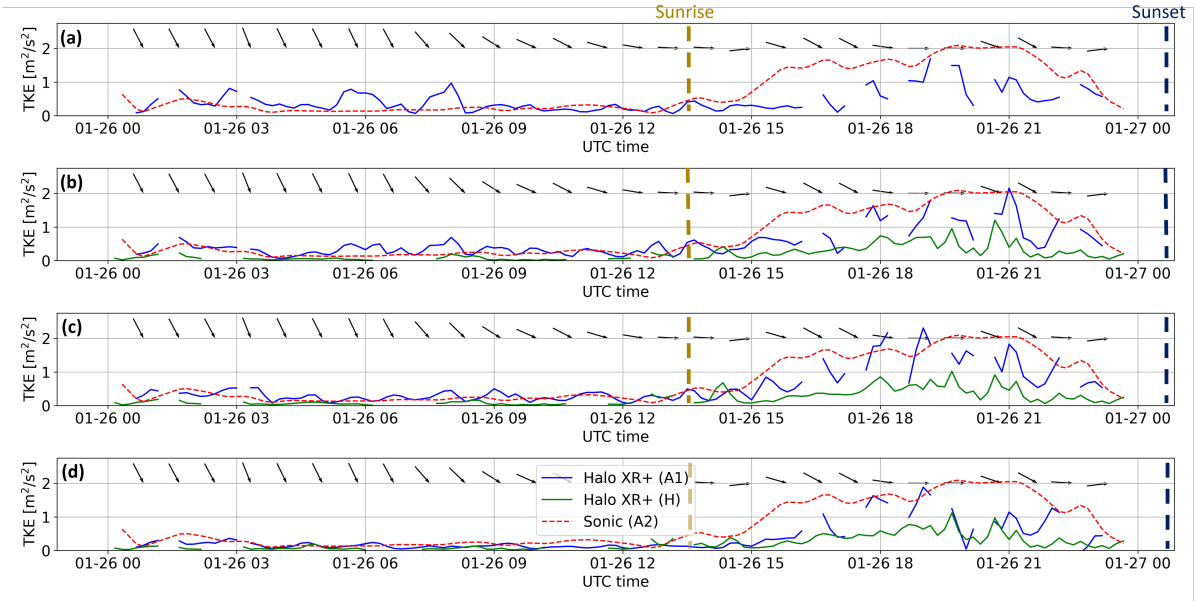

Figure 3. Turbulence kinetic energy retrieved from the lidars at (a) 100 m, (b) 150 m, (c) 200 m, and (d) 250 m above the ground, and the same quantity calculated from the 4-m sonic anemometer at site A2. The wind direction at $z = 100$ m is also reported for reference (black arrows).

The results from the scanning lidars, although qualitatively insightful, are possibly affected by the poor accuracy of the selected scanning approach, which assumes horizontal homogeneity of the flow, not expected to be valid in the presence of wakes. Therefore, the wake-generated turbulence is investigated more thoroughly through a comparative analysis of sonic data collected at multiple locations. Following the analysis of Bodini et al.[9], we calculate the percentage difference in TKE as measured by the 4-m sonic anemometers at site G (within the wind farm) and site A5 (outside the wind farm), as a function of wind direction (figure 4). We segregate results based on atmospheric stability, quantified in terms of the Obukhov length L, and consider stable conditions to be those when $0\,\text{m} < L \leq 200\,\text{m}$, and unstable conditions to be those when $-200\,\text{m} \leq L < 0\,\text{m}$. Also, to isolate periods when the King Plains turbines are expected to be operating, we only consider times when the 4-m wind speed is larger than 3 m/s. We see that near-surface TKE at site G is more than 50% larger than at site A5 in stable conditions for south-southwesterly wind directions, i.e., when site G is downwind of multiple rows of turbines and it is reasonable to expect a large impact of wakes. Conversely, a negligible difference in TKE is observed in unstable conditions when wakes dissipate much faster. We note how the wind direction sector highlighted in gray in figure 4 shows higher TKE at site A5 because of the impact of the wake of a shipping container deployed at that location. Once all instruments are deployed, a similar analysis will be refined by comparing sonic anemometer observations from a larger number of sites across the King Plains wind plant, and we will also assess near-surface impacts on different variables.

4. Simulations

A range of simulations have been performed for the AWAKEN experiment using large-eddy simulations in preparation for validation exercises for high-fidelity tools and more simple engineering models to help design the wind farm controls aspects of the AWAKEN project.

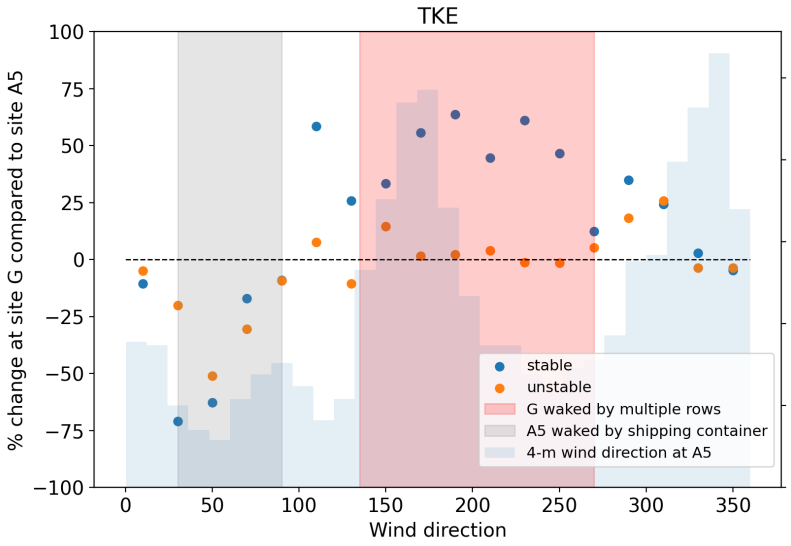

Figure 4. Mean percentage difference in 4-m sonic anemometer TKE between sites G and A5, for all 20-deg wind direction bins.

Researchers have performed large-eddy simulations of subsets and the entire AWAKEN domain using AMR-Wind [2], as seen in figure 5. These simulations, detailed in Cheung et al. [10], cover all five wind farms with a total of 541 turbines and installed rated power potential of more than 1.1 GW. These simulations are run under unstable atmospheric conditions and represent some of the largest wind farm simulations to date. The simulation domain is 100 km x 100 km x 2.5 km with a spatial resolution ranging from 2.5 m to 20 m and total mesh count of 21B cells. For the unstable ABL condition, a surface roughness of $z_0 = 0.15$m and surface temperature flux of 0.0442 K-m/s was chosen to match the shear and TI characteristics of an unstable 10 m/s hub-height condition as measured by nearby instrumentation. The initial flow-field was developed using a horizontally periodic precursor calculation which run for more than 5 hours, before starting the simulations with active wind turbines.

The simulation can be broken into individual wind farms as shown in figures 6 and 7, and the turbines in each wind farm are modeled through Joukowsi actuator disk models [11] (Thunder Ranch, Armadillo Flats, Chisholm View, and Breckinridge), or OpenFAST-coupled [12] actuator disks (King Plains). While the presence of individual turbine wakes is obvious in these simulations, larger wind farm wakes break down quickly under unstable conditions and are less obvious. We do expect longer larger wind farm wakes to be more predominant in the stable atmospheric boundary layer simulations. Additional analysis of the LES calculations, including averaged flow and power generation, can be found in [10], and all simulation parameters and results are available online [13].

One unique aspect of the AWAKEN campaign is the study of wind farm controls in a large wind farm. Wake steering, one of the wind farm control technologies investigated in the campaign, is a control strategy wherein upstream wind turbines are misaligned with the wind to deflect their wakes away from downstream turbines, which can increase total wind plant power [14]. In preparation for the wind farm control experiment, numerous simulations in the computationally efficient FLORIS engineering wind farm control modeling tool [3] have been used to design the wake steering controller. To model wake interactions and wake steering we use the Gauss-curl hybrid (GCH) model in FLORIS [15]. The GCH model combines the self-similar Gaussian wake deficit model discussed by Niayifar and Porté-Agel [16] and the

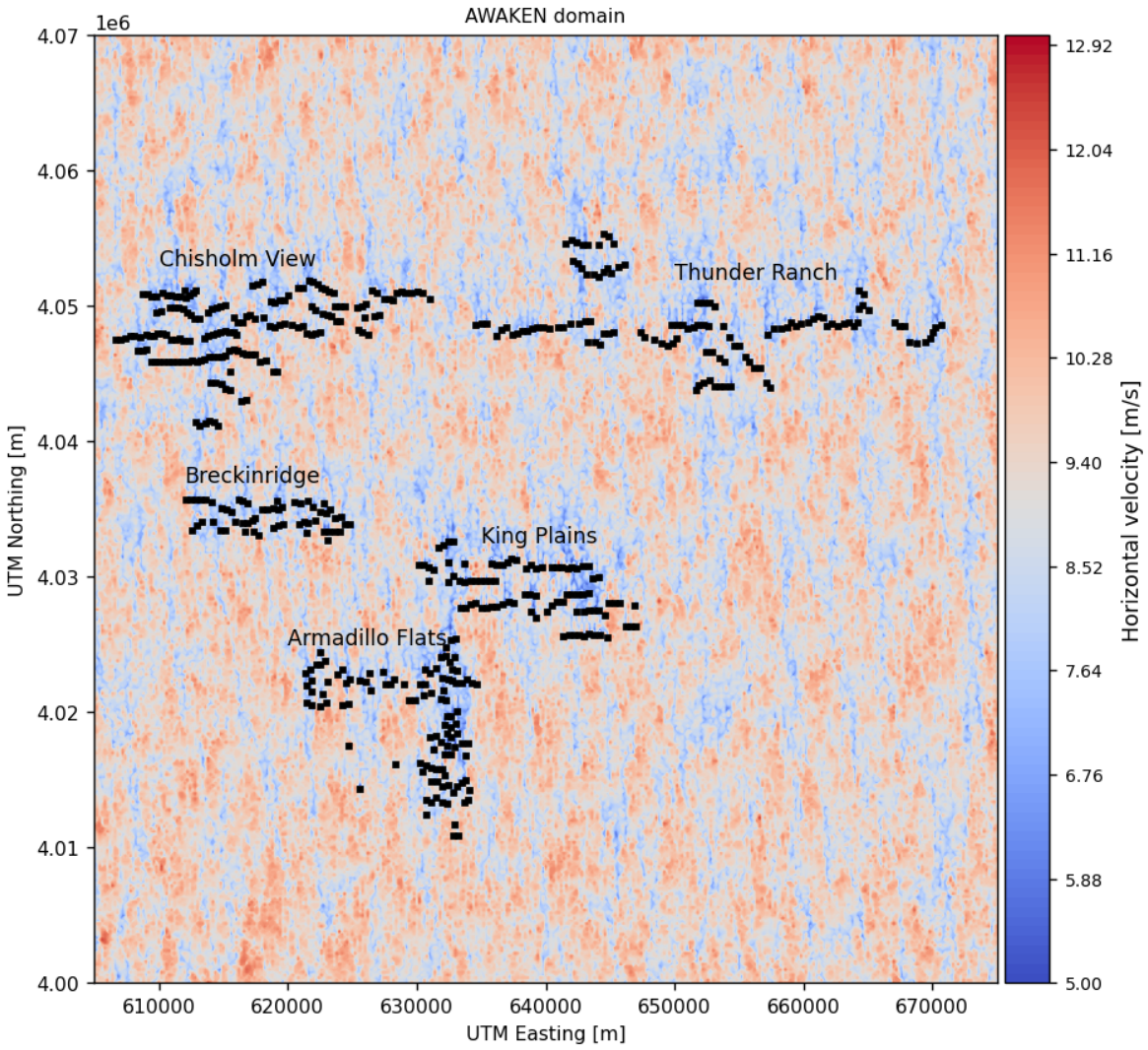

Figure 5. Contour of instantaneous horizontal velocity at the $z = 90$m plane for the five wind farms in the AWAKEN simulation domain.

wake deflection model presented by Bastankhah and Porté-Agel [17] with aspects of the curl wake model developed by Martínez-Tossas *et al.* [18], which captures the effects of large-scale trailing vortices caused by yaw misalignment on wake recovery and secondary steering (whereby the trailing vortices continue to deflect the wakes of downstream turbines with which they interact). Specifically, in FLORIS V2.5 [3], we use the "gauss_legacy" velocity deficit model, "gauss" deflection model, "crespo_hernandez" wake-added turbulence model, and "sosfs" wake combination model (with default parameters). The power loss from yaw misalignment is modeled in FLORIS by scaling the rotor effective wind speed by $(\cos\gamma)^{p_p/3}$, where γ represents the yaw misalignment and p_p is a user-defined power-loss exponent (we use a value of $p_p = 2$). Baseline FLORIS flow fields (i.e., without wake steering) for the subset of the King Plains wind plant where wake steering is implemented are shown in figure 8 for a wind speed of 8 m/s, wind direction of 180 degrees, and turbulence intensities of 5%, 8%, and 11%. The 15 wind turbines for which wake steering is implemented are circled. As turbulence intensity increases, the wakes

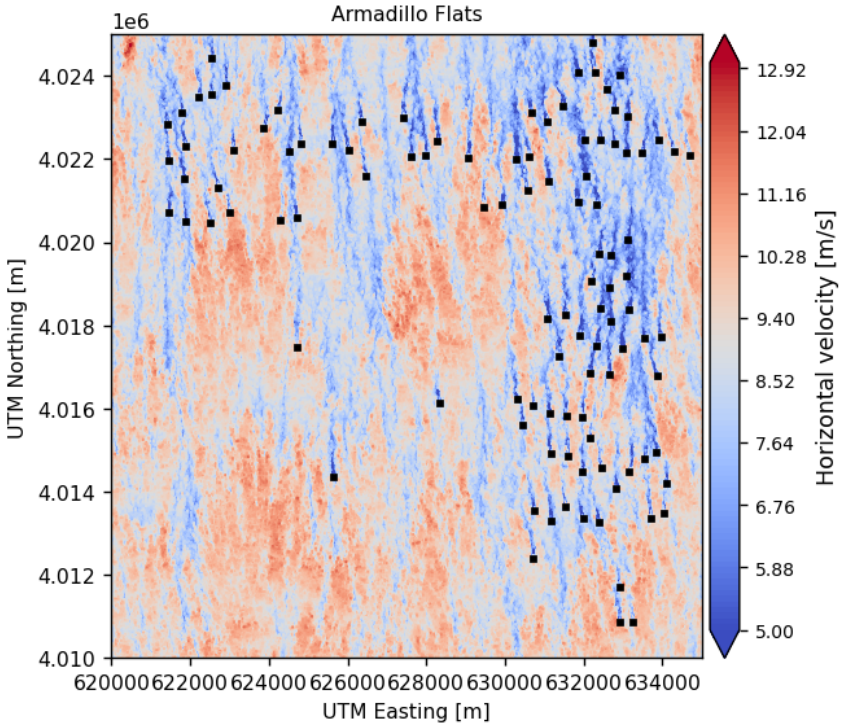

Figure 6. Instantaneous horizontal velocity at $z = 80$m hub-height plane showing the turbine wakes of the Armadillo Flats wind farm.

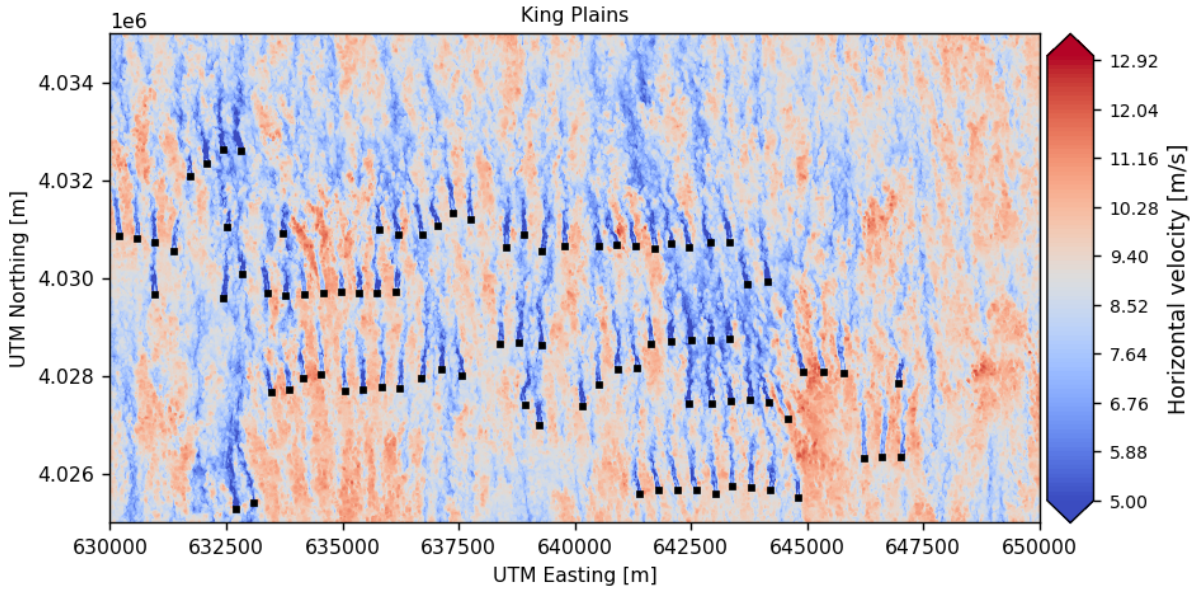

Figure 7. Instantaneous horizontal velocity at the $z = 90$m hub-height plane showing the turbine wakes of the King Plains wind farm.

recover faster, causing lower wake losses at downstream turbines.

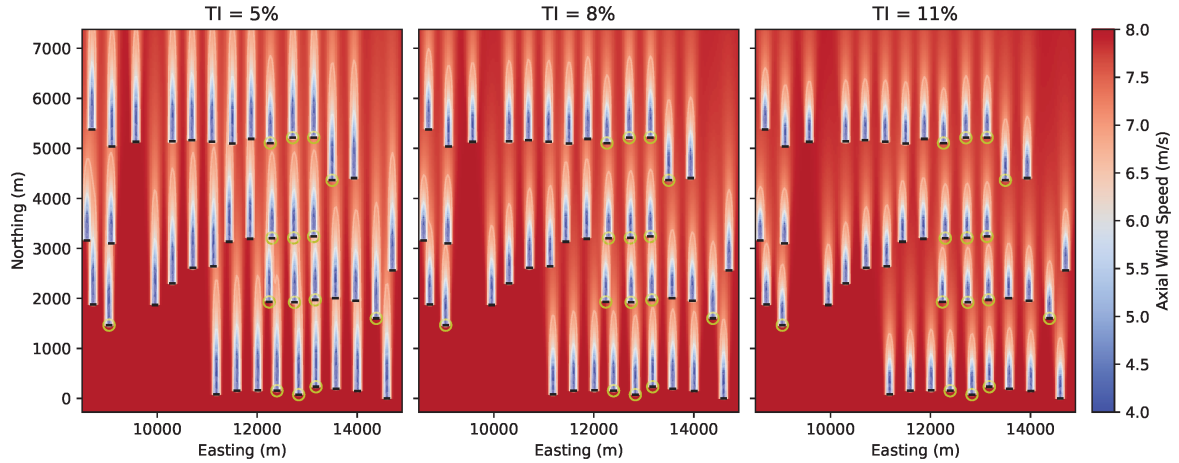

Figure 8. Streamwise velocity field a at hub height from FLORIS simulations at different ambient turbulence intensity (TI) levels.

Figure 9 shows the baseline wake losses and potential increases in energy production from wake steering in the experiment as a function of wind direction based on FLORIS simulations. The potential energy gains are found by using the Serial-Refine method [19] in FLORIS to identify the optimal yaw offsets for the set of wake steering turbines that maximize total wind plant power as a function of wind speed (in 1 m/s steps) and wind direction (in 1 degree increments). To allow safe operation, the yaw offsets are limited to between -24 degrees and $+24$ degrees at low wind speeds, and the maximum allowable offsets are reduced further as wind speed increases. Energy production with and without wake steering is found by summing the corresponding wind plant power values in each wind speed and wind direction bin by the long-term wind rose frequencies for King Plains based on 7 years of hourly data from the WIND Toolkit [20] wind resource data set. Note that the wake losses and energy gains are computed for the entire wind plant, but wake steering is only active for the 15 turbines on the east side of the plant shown in figure 8.

Figure 9 shows that the greatest benefits from wake steering arise for easterly and westerly directions where wake losses are highest because of the close turbine spacing. In general, larger wake losses provide more opportunity for wake steering to increase power production. Unfortunately, flow from the east and west is not that common. However, there is still benefit from wake steering in the most common wind direction from the south. Additionally, figure 9 reveals that wake losses as well as the predicted energy gains from wake steering are larger at lower turbulence intensities. Wakes persist longer as turbulence decreases, which causes greater power deficits at downstream turbines and thus greater potential for power gains from wake steering. Further, wakes are narrower when turbulence intensity is lower; therefore, wake deflection from wake steering has the potential to increase power more substantially at downstream turbines during periods with lower turbulence. Consequently, we expect low-turbulence conditions to provide the best opportunity to observe significant energy gains from wake steering during the experiment, especially when the wind is from the south.

5. Conclusions

The AWAKEN project represents one of the largest wind farm field campaigns to date that also includes wind farm control studies. Initial observations show a definitive presence of wakes from

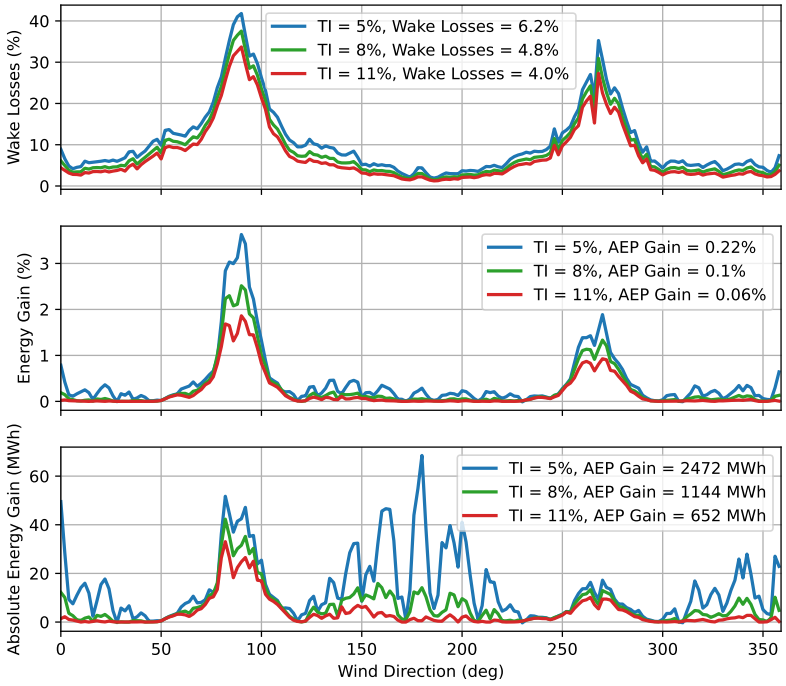

Figure 9. Baseline wake losses as well as relative and absolute energy gains from wake steering for the King Plains wind plant based on FLORIS simulations and yaw offset optimizations for turbulence intensities of 5%, 8%, and 11%. TI = turbulence intensity; AEP = annual energy production.

lidar measurements and also an increase in turbulence kinetic energy under stable conditions downwind of multiple rows of turbines. Initial simulations have been conducted in preparation for model validation studies and also to help design the wind farm control studies. The wind farm control studies show a potential energy gain dependent on inflow atmospheric turbulence intensity. Data are continuously streamed to the U.S. Department of Energy's Wind Data Hub [21] located at http://a2e.energy.gov. Benchmarks are being developed for the AWAKEN seven testable hypotheses that will be released for the benefit of the wind industry and research community alike.

Acknowledgments

This work was authored in part by the National Renewable Energy Laboratory, operated by Alliance for Sustainable Energy, LLC, for the U.S. Department of Energy (DOE) under Contract No. DE-AC36-08GO28308. Funding provided by the U.S. Department of Energy Office of Energy Efficiency and Renewable Energy Wind Energy Technologies Office. This research was supported by the Wind Energy Technologies Office of the U.S. Department of Energy (DOE) Office of Energy Efficiency and Renewable Energy. Sandia National Laboratories is a multimission laboratory managed and operated by National Technology & Engineering Solutions of Sandia, LLC, a wholly owned subsidiary of Honeywell International Inc., for the U.S. DOE's National Nuclear Security Administration under contract DE-NA0003525. A portion of this research was performed using computational resources sponsored by the U.S. Department of Energy's Office of Energy Efficiency and Renewable Energy and located at the National Renewable Energy Laboratory. This research also used resources of the Oak Ridge Leadership Computing Facility, which is a DOE Office of Science User Facility supported under Contract DE-AC05-00OR22725, which was provided through the ASCR Leadership Computing Challenge (ALCC) program.

References

[1] Moriarty P, Hamilton N, Debnath M, Herges T, Isom B, Lundquist J K, Maniaci D, Naughton B, Pauly R, Roadman J, Shaw W, van Dam J and Wharton S 2020 American WAKE experimeNt (AWAKEN) Tech. Rep. NREL/TP-5000-75789 National Renewable Energy Lab. (NREL), Golden, CO (United States) URL `https://www.nrel.gov/docs/fy20osti/75789.pdf`

[2] Sprague M A, Ananthan S, Vijayakumar G and Robinson M 2020 *Journal of Physics: Conference Series* vol 1452 (IOP Publishing) p 012071

[3] National Renewable Energy Laboratory 2022 FLORIS. Version 2.5 URL `https://github.com/NREL/floris`

[4] Lee J C and Fields M J 2021 *Wind Energy Science* **6** 311–365

[5] Krishnamurthy R, Newsom R K, Chand D and Shaw W J 2021 Boundary Layer Climatology at ARM Southern Great Plains Tech. Rep. PNNL-30832 Pacific Northwest National Lab. (PNNL), Richland, WA (United States) URL `https://www.osti.gov/biblio/1778833`

[6] Moriarty P, Bodini N, Brugger P, Goldberger L, Hamilton N, Herges T, Hirth B, Iungo G V, Ivanov H, Kaul C, Klein P, Krishnamurthy R, Letizia S, Lundquist J K, Morris V R, Newsom R, Pekour M, Porté-Angel F, Scholbrock A, Schroeder J, Simley E, Wharton S and Zalkind D 2023 *Journal of Renewable and Sustainable Energy - submitted January 2023*

[7] Sathe A, Mann J, Vasiljevic N and Lea G 2015 *Atmospheric Measurement Techniques* **8** 729–740 ISSN 18678548

[8] Beck H and Kühn M 2017 *Remote Sensing* **9** ISSN 20724292

[9] Bodini N, Lundquist J K and Moriarty P 2021 *Scientific Reports* **11** ISSN 2045-2322 URL `https://www.nature.com/articles/s41598-021-02089-2`

[10] Cheung L 2023 *IOP Conference Series - Wake Conference 2023 - submitted April 2023*

[11] Van Kuik G 2022 *The Fluid Dynamic Basis for Actuator Disc and Rotor Theories: Revised Second Edition* (IOS Press)

[12] National Renewable Energy Laboratory 2023 OpenFAST URL `https://github.com/OpenFAST/`

[13] US Department of Energy Wind Data Hub URL `http://a2e.energy.gov` - *accessed April 2023*

[14] Boersma S, Doekemeijer B M, Gebraad P M O, Fleming P A, Annoni J, Scholbrock A K, Frederik J A and Wingerden J W V 2017 *Proc. American Control Conference* (Seattle, WA, USA) pp 1–18 ISBN 978-1-5090-5994-2

[15] King J, Fleming P, King R, Martínez-Tossas L A, Bay C J, Mudafort R and Simley E 2021 *Wind Energy Science* **6** 701–714

[16] Niayifar A and Porté-Agel F 2016 *Energies* **9**

[17] Bastankhah M and Porté-Agel F 2016 *Journal of Fluid Mechanics* **806** 506–541

[18] Martínez-Tossas L A, Annoni J, Fleming P A and Churchfield M J 2019 *Wind Energy Science* **4** 127–138

[19] Fleming P A, Stanley A P J, Bay C J, King J, Simley E, Doekemeijer B M and Mudafort R 2022 *Journal of Physics: Conference Series* **2265** 032109

[20] Draxl C, Hodge B M, Clifton A and McCaa J 2015 Overview and meteorological validation of the Wind Integration National Dataset Toolkit Tech. Rep. NREL/TP-5000-61740 National Renewable Energy Laboratory

[21] Macduff M and Sivaraman C 2017 *AGU Fall Meeting Abstracts* vol 2017 pp GC13J–0877